Am J Clin Exp Immunol 2013;2(2):172-185
www.ajcei.us /ISSN:2164-7712/AJCEI1305001

Original Article

The oxidase activity of vascular adhesion protein-1 (VAP-1) is essential for function

Thomas Noonan, Susan Lukas, Gregory W Peet, Josephine Pelletier, Mark Panzenbeck, Adedayo Hanidu, Suzanne Mazurek, Ruby Wasti, Irina Rybina, Teresa Roma, Anthony Kronkaitis, Alycia Shoultz, Donald Souza, Huiping Jiang, Gerald Nabozny, Louise Kelly Modis

Boehringer Ingelheim Pharmaceuticals, 900 Ridgebury Road, Ridgefield, CT 06877

Received May 14, 2013; Accepted May 29, 2013; Epub June 15, 2013; Published June 30, 2013

Abstract: Vascular adhesion protein-1 (VAP-1) has been implicated in the pathogenesis of inflammatory diseases and is suggested to play a role in immune cell trafficking. It is not clear whether this effect is mediated by the oxidase activity or by other features of the protein such as direct adhesion. In order to study the role of VAP-1 oxidase activity *in vivo*, we have generated mice carrying an oxidase activity-null VAP-1 protein. We demonstrate that the VAP-1 oxidase null mutant mice have a phenotype similar to the VAP-1 null mice in animal models of sterile peritonitis and antibody induced arthritis suggesting that the oxidase activity is responsible for the inflammatory function of VAP-1.

Keywords: Vascular adhesion protein-1 (VAP-1), semicarbazide-sensitive amine oxidase, immune cell trafficking, oxidase activity, inflammatory function

Introduction

Vascular adhesion protein-1 (VAP-1) has been suggested to play a role in immune cell trafficking and has been implicated in the pathogenesis of inflammatory diseases including arthritis, multiple sclerosis, diabetes and atherosclerosis by influencing immune cell trafficking (via cell adhesion) and cell activation [1-5]. It is therefore a target of interest for autoimmune, inflammatory and fibrotic diseases and BIOTIE therapeutics is conducting Clinical trials with their anti-VAP-1 antibody. Several small molecule inhibitors have also been described [6, 7]. VAP-1 is expressed at significant levels on endothelial cells, adipose tissue, smooth muscle cells and is also found on pericytes and follicular dendritic cells [2, 8]. However, its mechanism of action as an immune modulator and its structure-function relationship is not clearly understood.

VAP-1 is a 180 kD glycoprotein also known as semicarbazide-sensitive amine oxidase (SSAO) or copper-containing amine oxidase (AOC 3, EC 1.4.3.6) that catalyzes oxidative deamination of primary amines. The enzymatic function has been studied using non-physiological substrates such as benzylamine. The active site of SSAOs contains an essential topoquinone (TPQ) cofactor, which is modified from tyrosine in a copper dependent manner, and so these enzymes are also called copper containing oxidases. The enzymatic reaction involves reduction of the primary amine with formation of a transient Schiff base via the TPQ with the release of an aldehyde. The reduced TPQ is then hydrolyzed with oxygen and subsequently hydrogen peroxide and ammonia are released. Mutation of this Tyrosine to Phenylalanine creates an oxidase dead version of the protein which is thought to be structurally intact and which leads to reduced leukocyte rolling and transmigration [9]. It has been suggested that VAP-1 can bind primary amines of proteins expressed on the cell surface and mediate a transient adhesion effect. The endogenous substrates are not all known, but it can oxidize methylamine and aminoacetone which are found in circulation and other substrates, such as Siglec 10 expressed on leukocytes [10] and Siglec 9 [11], have recently been described.

In order to effectively target VAP-1, it is important to understand what are the critical functions to inhibit; whether it is necessary to block

protein binding or enzymatic function or both. Here, through the generation and characterization of mice which express VAP-1 without oxidase activity, we show that their phenotype is comparable to that seen with mice that lack VAP-1 protein completely and extend observations from *in vitro* experiments [9] demonstrating a role in leukocyte adhesion and transmigration.

Methods

Generation of KI mice

The VAP-1^{Y471F} founder mice were generated by TaconicArtemis GmbH (Cologne, Germany) for Boehringer Ingelheim and genotyped as described in the supplemental information.

Tissue preparation

Mice were anesthetized with inhaled isoflurane (Baxter Healthcare, Deerfield, IL) with a VetEquip anesthesia machine, blood was obtained by axillary bleed in citrate microcentrifuge tubes (Eppendorf) and the mice were sacrificed. The left atrium was cut and the lungs were perfused free of blood with 4-5 mL of cold phosphate buffered saline (PBS, Gibco) via the right ventricle. The thoracic aorta and the abdominal aorta to the renal arteries were removed. Abdominal fat pads were removed. Tissue was homogenized using a Fast-Prep 24 (MP biomedicals, Solon, OH) All tissue was placed in weighed, pre-chilled tissue homogenization tubes (Lysing Matrix D), snap frozen in liquid nitrogen and stored at -70°C. For assay of tissue amine oxidase activity and western analysis, ice cold assay buffer (see VAP-1 oxidase assay below) was added in weight/volume ratios of 1:4 for lung and adipose tissue and 1:8 for aorta. The tissue was processed twice for 30 seconds and the homogenate was centrifuged at 13,000 rpm in a Beckman microfuge at 4°C. The supernatant was removed and quantified for total protein using Coomassie Plus™ Protein Assay Reagent from Thermo Scientific (Rockford, IL) according to the manufacturer's instructions.

Western analysis

Samples (10 µg/lane) were run on a 4-12% Bis-Tris gel from Invitrogen (Carlsbad, CA) using MES SDS buffer, and transferred to nitrocellulose (0.45 µm) using semi-dry blotting (OWL Scientific, San Francisco, CA) at 200 mAmps for 1 hour at room temperature. The membrane was blocked overnight at 4°C with Li-Cor Blocking buffer (Odyssey Cat No. 927-40000, Lincoln, NE) containing 0.1% Tween-20. Primary antibodies were anti-murine VAP-1 (Cat. #V84120-050 BD Transduction Labs, San Jose, CA) at 1:250 and anti-β-tubulin (Cat. #sc-9104 Santa Cruz Biotechnology, Inc.) at 1:100. Secondary antibodies were goat anti-mouse IgG IR Dye 800 CW (Li-Cor cat. #926-32210) and goat anti-rabbit IgG IR Dye 680 (Licor cat. #926-32221) both used at 1:2000 dilutions. Densitometric signals at ~85 kD and ~50 kD were quantified on Li-Cor Odyssey Scanner software. Quantitative values were then given for each adipose sample normalized to β-tubulin.

TaqMan real-time quantitative PCR

Reverse transcription (RT) reactions were carried out for each RNA sample in strip-well tubes using reagents from the TaqMan reverse transcription reagents kit (cat #N808-0234, ABI). Each reaction tube contained 1000 ng of total RNA in a volume of 50 µL containing 1 x TaqMan RT buffer, 5.5 mM $MgCl_2$, 500 mM of each dNTP, 2.5 mM of Random Hexamers, 0.4 U/mL of RNase inhibitor, and 1.25 U/mL of MultiScribe Reverse Transcriptase. RT reactions were carried out at 25°C for 10 min, 48°C for 40 min and 95°C for 5 min [Note: the incubation at 25°C for 10 min is necessary for the RT reaction with random hexamers to obtain optimal results]. Upon completion of reverse transcription, the RT reaction mixture was brought up to a final volume of 100 µL by diluting with 50 µL RNase-free water, and then placed at 4°C for immediate use in PCR amplification, or stored at -20°C for later use (similar results are expected at these two different storage temperatures). Probes for VAP-1 (Mm00839624_m1), AOC 1 (Mm00504051_m1), AOC 2 (Mm00841716_m1) and GAPDH (Mm99999915_g1) were purchased from Applied Biosystems. A thermal stable AmpliTaq Gold DNA polymerase was used for the PCR amplification. Real-time PCR was performed in a MicroAmp Optical 384-Well Reaction Plate (Applied Biosystems). Each well contained 20 ng total RNA), 5.5 mM $MgCl_2$, 200 mM dATP/dCTP/dGTP, 400 mM dUTP, 1 x TaqMan assay-on-demand probe mix,

0.01 U/mL AmpErase, and 0.025 U/mL AmpliTaq Gold DNA polymerase. Amplification conditions were 2 min at 50°C (for AmpErase UNG incubation to remove any uracil incorporated into the cDNA), 10 min at 95°C (for AmpliTaq Gold activation), and then run for 40 cycles at 95°C for 15 s, 60°C for 1 min. All reactions were performed in the ABI 7900HT Sequence Detection System for the reference, test samples and no template controls. They were run in triplicates using the Sequence Detector V 2.3 program. The *R*n and *C*t were averaged from the values obtained in each reaction.

Recombinant protein production

Human VAP-1 (41-755) and VAP-1^{Y471F} (41-755) with a mutated GST N-terminal fusion tag (with Cysteines at position 85, 138, and Serine at position 178) were expressed in pcDNA-Dest40 Gateway Vector (Invitrogen, Carlsbad, CA). The native signal sequence was replaced with a murine IgG heavy chain signal peptide and a HRV protease cleavage site was introduced after the mutated GST fusion tag. HEK 293 cells were transfected with the expression vectors for VAP-1 using Freestyle MAX (Invitrogen) transfection reagent according to the manufacturer's protocol and selected with 500 μg/mL G418 (Invitrogen). Human VAP-1 (41-755) was expressed in pools of stably expressing cells as described [12]. VAP-1^{Y471F} (41-755) was transiently expressed using 293fectin (Invitrogen) in HEK 293F cells which were harvested after 120 hrs. Both VAP-1 proteins were purified from fresh biomass by affinity chromatography using Glutathione Sepharose 4B resin (Amersham Biosciences) in the presence of 0.1% TWEEN-20 as described [12].

VAP-1/AOC oxidase assay

The AOC luminescence assay is based on the MAO-Glo Assay (Cat. #V1401, Promega Technical bulletin 2007 Instructions for use of products V1401 and V1402. [Part #TB345. http://www.promega.com/tbs/tb345/tb345.pdf and 12]). The assay buffer was modified from the "physiological HEPES" [13] and consisted of 50 mM HEPES pH 7.4, 5 mM KCl, 2 mM $CaCl_2$, 1.4 mM $MgCl_2$, 120 mM NaCl, 0.001% Tween 20, and 100 μM TCEP (Thermo Scientific, Rockford, IL). Catalysis reactions ranged from 60 mins (recombinant protein with 27 μM substrate) -120 min (aorta and adipose tissue and 1 nM recombinant WT control material with 20 μM substrate) 37°C followed by a 20 min 37°C detection reaction, after which Relative Light Units were counted on an LJL BioSystems Analyst AD (Molecular Devices, Sunnyvale, CA). The Promega MAO-Glo substrate was solubilized as a 16 mM 100% DMSO stock. This resulted in a ≤ 0.5% DMSO contribution from the substrate after dilution into the assay, depending on the substrate concentration. Assay plates were from Greiner (Cat. #655075). The compound inhibitor was solubilized in 100% DMSO, and serially diluted in 100% DMSO prior to being diluted into assay buffer and added to the plate resulting in 1% final DMSO that was mimicked in control and background samples. Adipose homogenate (26 μg) was pre-incubated for 20 min at 37°C with varying concentrations of the compound of interest plus 1 μM each of clorgyline & deprenyl prior to initiating the assay with 23 μM substrate and carrying out the Standard Assay (60 min catalysis). Background with no homogenate or compound of interest, plus clorgyline and deprenyl was subtracted from each sample. The IC_{50} curve was generated by SigmaPlot regression fitting using the Equation Category "Sigmoidal" and the Equation Name "Hill 3 Parameter".

Assessment of leukocyte profile

Citrate anticoagulated blood was tested for white blood count, hematocrit and differentials using a Beckman Coulter AcT Diff Coulter Counter for WT and VAP-1^{Y471F} mice (n=10/group, respectively). White blood cell counts and differentials were reported as mean ± SD (x 10^{-3}/μL) and lymphocyte, granulocyte and monocyte differentials were as mean ± SD (x 10^{-3}/μL) and as a percent; hematocrits were also reported as a percent. Statistical analysis was performed using the unpaired Student's *t* Test.

Flow cytometry

Spleen and bone marrow from femurs and tibias of four 8-10 week old naïve WT and four VAP-1^{Y471F} mice were prepared as a single cell suspension by passing through 100 μm mesh (Becton Dickinson), washing with 10 mL cold Dulbecco's modified Eagles medium (DMEM, Gibco), then passing through a 40 μm mesh fil-

ter. The filtered washed cells were centrifuged at 600Xg and resuspended in 2 mL FACS buffer (0.5% bovine serum albumin, 0.1% sodium azide (Sigma, St. Louis) with 10 μg/mL Fc blocking antibody (anti-CD16/CD23 BD Pharmingen, clone 2.4G2). Cell counts were performed in a Coulter Z2 counter, and FACS buffer with FC block was added to bring the cell concentration to 3-7 x 10^6 cells/mL.

For analysis of spleen lymphocytes, nine aliquots of 70 μL were placed in 96 well round bottom plates for each sample. To one of each of the wells was added 70 μL of FACS buffer or the following antibodies each at 5 μg/mL: anti-CD3-FITC (eBioscience clone 145-2C11), anti-CD4-PE (eBioscience, clone GK1.5), anti-CD8-PerCP-Cy5.5 (BD Pharmingen, clone 53-6.7), anti-CD19-APC-Cy7 (BD Pharmingen, clone 1D3), all four antibodies combined, all 4 isotype control antibodies combined, (eBioscience Armenian hamster IgG-FITC, rat IgG2b κ-PE, rat IgG2a-κ-PerCP-Cy5.5, rat IgG2a-κ-APC-Cy7, respectively), CD45-PE (BD Pharmingen, clone 30-F11), and individual isotype control IgG2b-κ-PE.

Bone marrow cells were aliquotted and stained for CD45 and lymphocytes as above and an additional six aliquots were plated and stained as follows: To one of each of the wells was added 70 μL of FACS buffer or the following antibodies each at 5 μg/mL: anti-F4/80- FITC (eBioscience clone BM8), anti-GR-1-PE (eBioscience clone RB6-8C5), anti-CD115-APC (eBioscience clone AFS98), all three antibodies combined, and combined isotype control antibodies (eBioscience rat IgG2b κ-PE, rat IgG2a κ-FITC, rat IgG2a κ-APC, respectively). For both staining protocols, after binding for one hour, the cells were washed twice with FACS buffer, resuspended in 100 μL PBS, fixed with 100 μL 2% paraformaldehyde, and stored at 4°C until analyzed on a Becton Dickinson LSRII flow cytometer. Cell percentages were multiplied by total cell counts to determine absolute numbers of each cell type. Leukocytes were selected by gating on CD45 staining. Lymphocytes falling in regions consistent with $CD45^+$ cells were gated as either T cells ($CD3^+$) or B cells ($CD19^+$). $CD3^+$ cells were further subdivided into $CD4^+$, $CD8^+$, or $CD4^+$ and $CD8^+$. Myeloid cells falling in regions consistent with $CD45^+$ cells were further defined as polymorphonuclear leukocytes (neutrophils, PMNs) by positive staining for GR-1 but not F4/80 or CD115. Macrophages were found to stain with F4/80 and in some cases also GR-1 or CD115. All F4/80 positive cells were defined as macrophages. Monocytes were defined as positive for macrophage colony stimulating factor (c-fms) or CD115 but F4/80 negative to avoid duplicate counting. From bone marrow there were populations that were CD115 and GR-1 positive, which are bone marrow monocytes [14, 15] and were included in monocyte counts. For acute peritonitis studies, washed peritoneal cells were resuspended in FACS buffer containing 10 μg/mL of Fc blocking antibody (anti-CD16/CD32). Six aliquots of 70 μL were placed in 96 well round bottom plates for each sample. To one of each of the wells was added 70 μL of FACS buffer or the following antibodies each at 5 μg/mL: anti-GR-1-PE (eBioscience clone RB6-8C5), anti-F4/80-FITC (eBioscience clone BM8), anti-CD115-APC (eBioscience clone AFS98), all three antibodies combined, individual isotype control antibodies (eBioscience rat IgG2b μ-PE, rat IgG2a μ-FITC, rat IgG2a μ-APC, respectively), and combined isotype control antibodies. For chronic peritonitis studies, washed peritoneal cells were resuspended in FACS buffer containing 10 μg/mL of Fc blocking antibody (anti-CD16/CD32). In addition to aliquots listed above for acute peritonitis, additional cells were stained for CD45 and separately for CD3, CD19, and for confirmation, CD115. Gating for cell definition was as above. Negligible CD3 positive cells were found in both naïve and thioglycollate induced peritonitis and were not reported. After staining with the antibodies as listed above, all cells were washed twice with FACS buffer, resuspended in 100 μL PBS, fixed with 100 μL 2% paraformaldehyde, and stored at 4°C until analyzed on a Becton Dickinson LSRII flow cytometer.

Peritonitis

Acute peritonitis was induced by intra-peritoneal injection of 0.5 mL of 3% Brewers modified thioglycollate (BBL, Lot No. 8252207) prepared according to the manufacturer's instructions. Four hours later, the mice were anesthetized by inhaled isoflurane, sacrificed by cervical dislocation and the peritoneal space lavaged with 7 mL of cold phosphate saline buffer with 1% fetal bovine serum albumin (Invitrogen) and 1 μM sodium EDTA (Sigma, St. Louis). The recovered lavage was placed on ice, centrifuged at

600Xg at 4°C, the supernatant decanted and resuspended in 2 mL FACS buffer with 10 μg/mL Fc blocking antibody (see above). Cell counts were determined on each sample using a Coulter Z1 counter, model 0034. For acute TNFα-induced peritonitis, the stimulus was an intra-peritoneal injection of 50 ng TNFα (R & D Systems, 410-MT), lavage was performed six hours after injection, and all other procedures were the same as above. Chronic peritonitis was induced by injection of 0.5 mL of 3% Brewer's modified thioglycollate medium. Three days later, the mice were lavaged and cells washed and counted as described above. There were 10 mice per group. The statistical tool used was a Student's T-test.

Anti-type II collagen antibody induced arthritis (CAIA)

Prior to experimentation, all animal procedures were in compliance with and approved by the BIACUC. An acclimation period of at least five days was observed before initiating the experiment. Animals were housed using paper bedding, constant humidity and temperature, a twelve hour light dark cycle with food and water provided *ad libitum*. Female C57BL/6 VAP-1 enzyme dead knock-in (VAP-1^{Y471F}) mice and WT C57BL/6 female mice were 9-11 weeks of age at the start of the experiment (n=10 per group). On day 0, mice were given an intra-peritoneal (I.P.) injection of 8 mg Arthrogen CIA mAb blend (Chemicon International). On the morning of day 3, 50 μg of LPS was injected I.P. To prevent dehydration resulting from endotoxin administration, mice were given 0.5 mL lactated ringers (at 37°C) subcutaneously on the afternoon of day 3. Disease progression and severity were assessed via a visual scoring system from day 3-14. Each limb was graded as follows: 0, normal; 1, edema in 1-2 digits; 2, edema in > 2 digits or mild edema about the tibiotarsal joint; 3, moderate edema to include the metatarsals; 4, maximal edema to include the metatarsals and phalanges. The clinical score per paw was summed to give a maximal severity score of 16 for each animal. Body mass was monitored on days 0, 3, 5, 7, 10, 12, and 14. On day 14, under deep anesthesia, blood was collected via cardiac puncture for serum analysis, mice were sacrificed, lung and aorta tissues excised and frozen, and paws collected in 10% neutral buffered formalin.

For graphing, group mean and standard error of the mean values were generated for both clinical score and body mass on days when data were recorded. Four paw summed values were used to generate area under the curve (AUC) values reflecting the clinical score with respect to time for each animal. To determine significance, AUC values from all members of a treatment group were tested against those of the vehicle control group by the Mann Whitney test using α=0.05. Percent inhibition was calculated for each treatment group by subtracting the treatment group mean AUC from the vehicle control mean AUC, dividing this difference by the vehicle control mean AUC value and multiplying the quotient by 100.

Results

Generation of VAP-1^{Y471F} mice

We generated mice that expressed an enzyme dead version of VAP-1 by making a tyrosine to phenylalanine mutation in exon 1 of VAP-1 through homologous recombination in ES cells to create a constitutive VAP-1^{Y471F} allele (**Figure 1A**). The point mutation (TAT to TTT) was introduced by PCR and the selectable marker gene was flanked by frt sites, which allowed it to be removed in ES cells before chimeric mice were generated. The introduction of the mutation was verified by sequencing the Su0053 construct and mice were genotyped by PCR using primers that spanned the remaining frt site (**Figure 1B**). The VAP-1^{Y471F} mice were healthy and fertile and were produced at Mendelian frequencies.

In order to verify that the mice expressed VAP-1 protein, we performed western analysis on adipose tissue (**Figure 2A**) and aorta (data not shown), as both tissues were previously described as having high levels of VAP-1 [16]. The protein concentration was calculated and lysate corresponding to 10 μg protein was resolved. A band which crossreacted with the anti-VAP-1 antibody is highlighted at 85 kDa and the expression was normalized to the β Tubulin band for each sample. The average ratio for VAP-1 to β-tubulin is 2.2 +/- 0.9 (standard deviation) in wild type mice and is 2.9 +/- 1.2 in VAP-1^{Y471F} mice confirming normal expression of VAP-1 in the VAP-1^{Y471F} mice. Similar results were obtained with western blots of aorta.

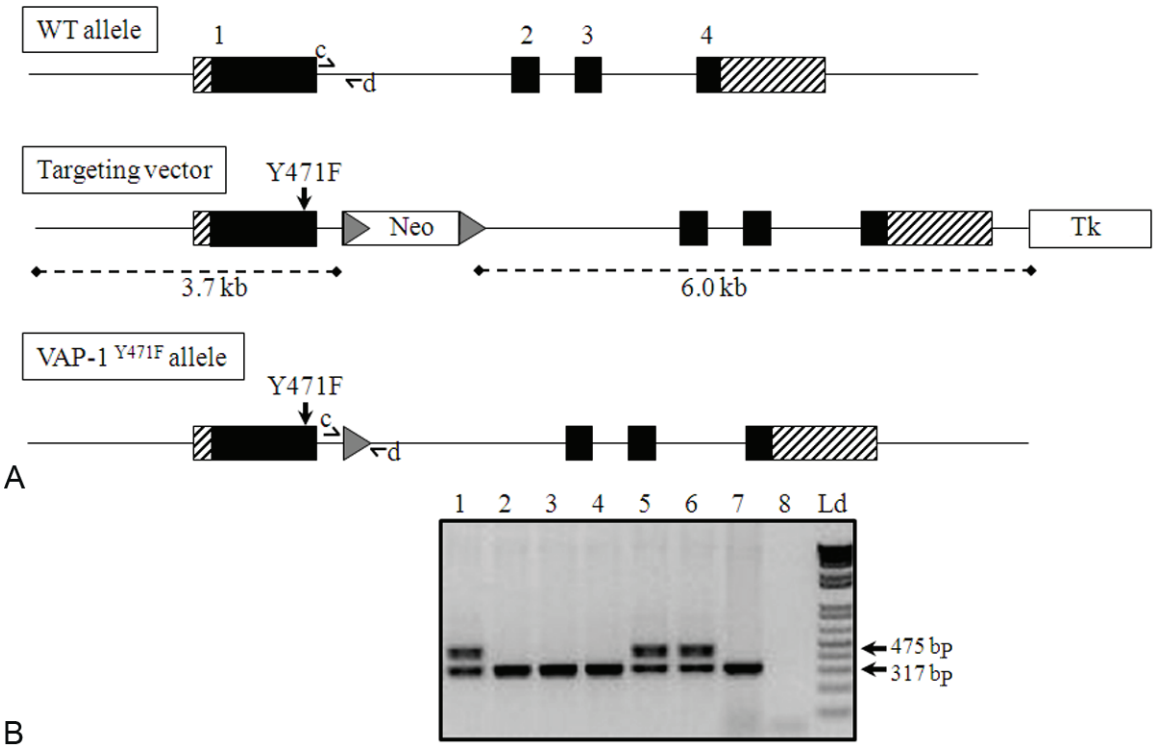

Figure 1. Generation of VAP-1^{Y471F} mice. A: Schematic representation of the wild type (WT) VAP-1 locus, the targeting vector Su0053 and the targeted VAP-1^{Y471F} allele after Flp recombination. The exons are indicated by numbers (1-4) on the WT locus and by boxes (solid black for coding and hatched for non coding). 5' and 3' genomic DNA and introns are shown as solid black lines. The Neomycin and thymidine kinase cassettes are shown as a white box and FRT sites are shown as grey triangles. The Y471F mutation is indicated in exon 1 and the short and long homology arms of the targeting vector are shown as a dashed line with the lengths indicated. The VAP-1^{Y471F} allele with the primers used for PCR genotyping is shown as black bars labelled 'c' and 'd'. B: PCR analysis of genomic DNA. Lanes 1-7 show the PCR results from 6 mice in the colony. Lane 7 is a wild type control, lane 8 is no DNA control and the DNA ladder is indicated by 'Ld'. The sizes of the fragments amplified are indicated, 475 bp and 317 bp.

As exon 1 of the VAP-1 gene is 1 kb downstream from the AOC 2 gene, we examined the mRNA expression of AOC 2 in adipose tissue (**Figure 2B**), lung and aorta (data not shown). The VAP-1 gene expression is comparable between the wild type and VAP-1^{Y471F} mice. AOC 2 gene expression is at lower levels than VAP-1 and is also comparable between wild type and the VAP-1^{Y471F} mice with relative expression levels at 7 and 5. AOC 1 was also analyzed in these samples and was at the limit of detection (data not shown). It is important to understand the relative levels of related oxidases in the tissues before evaluating the enzyme activity levels of VAP-1^{Y471F} as all three enyzmes can use benzylamine as a substrate.

Prior to generating the VAP-1^{Y471F} mice, we confirmed that the VAP-1^{Y471F} protein was indeed enzymatically inactive in a bioluminescent assay (described in the Materials and Methods) and as reported [9]. Recombinant truncated wild type VAP-1 (41-755) protein (described in Materials and Methods) gave robust activity in the assay whereas the VAP-1^{Y471F} protein showed activity comparable to background, even under conditions of 200 nM protein (40 X what is required for wild type activity) (**Figure 3A**). Tissue samples from wild type and VAP-1^{Y471F} mice either aorta (**Figure 3B**) or adipose (**Figure 3C**) were prepared and assayed as described (Materials and Methods). In both cases, the wild type tissue homogenate gave robust activity with adipose tissue showing higher oxidase activity than aorta, while VAP-1^{Y471F} tissue homogenate displayed activity similar to background. 1 nM of recombinant VAP-1 (41-755) was assayed in parallel as a positive control. Clorgyline and deprenyl were added in order to inhibit any non-specific MAO-A and MAO-B signal. Finally, adipose tissue homogenate from 9 wild type mice (used in **Figure 3C**)

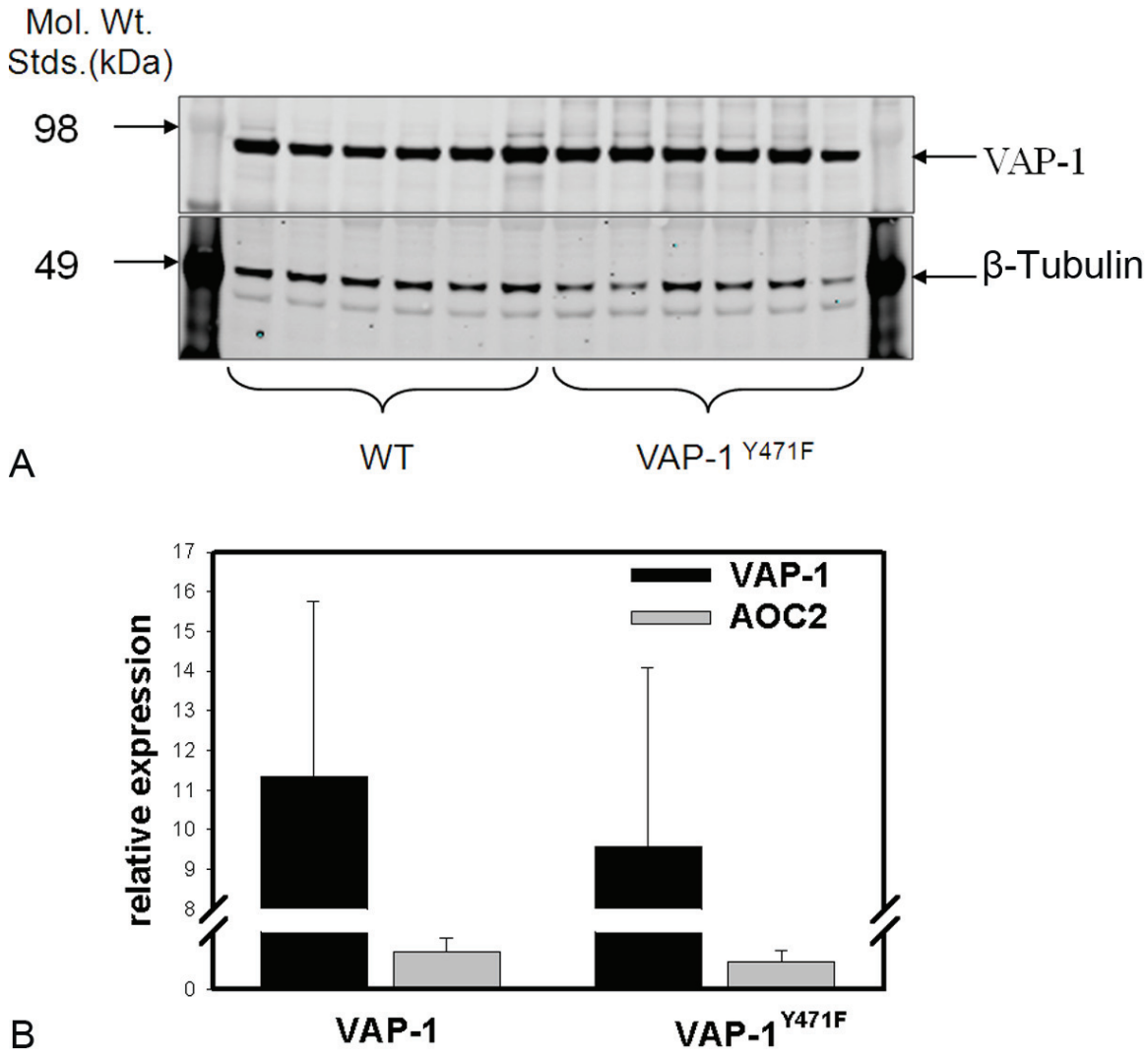

Figure 2. VAP-1 and AOC 2 expression in VAP-1^{Y471F} mice. A: Western blot analysis of adipose tissue from 6 wild type VAP-1 (WT) and 6 VAP-1^{Y471F} mice. The upper panel shows the blot probed for VAP-1 and the lower panel shows the same blot which was probed for βTubulin. The VAP-1 and βTubulin bands are indicated with arrows in each case. The molecular weight standard is indicated by Mol. Wt. Stds (kDa) and the 98 and 49 kDa bands are highlighted. B: Quantitative PCR on 20 ng of cDNA generated from adipose tissue from wild type VAP-1 (WT) and VAP-1^{Y471F} mice. VAP-1 is indicated with a black bar and AOC 2 is indicated with a grey bar. The relative expression of each of the genes to GAPDH is shown on the x axis. The data represents an average of 9 wild type and 8 VAP-1^{Y471F} mice and the standard deviations are shown with error bars.

was pooled to prepare a uniform sample in order to assay with a specific VAP-1 inhibitor. LJP 1586, in a 10 point dose response curve to generate an IC_{50} of 15.4 nM (**Figure 3D**) as reported [7]. This further confirmed that the response measured in **Figure 3C** is indeed VAP-1 activity.

Phenotype of VAP-1^{Y471F} mice

VAP-1^{Y471F} mice were viable, born at Mendelian frequencies and bred normally. They appeared healthy, with the only notable difference being a slight tendency of being overweight, particularly noticed in the males. Similar to what has been published for the VAP-1 null mice [17], there were no differences between wild-type (WT) and the VAP-1^{Y471F} mice in peripheral total white blood cell counts (**Table 1**). There were also no significant differences between WT and VAP-1^{Y471F} mice in circulating lymphocytes, granulocytes, platelets, or erythrocytes. The number of monocytes in peripheral blood was not significantly greater in VAP-1^{Y471F} vs. WT mice

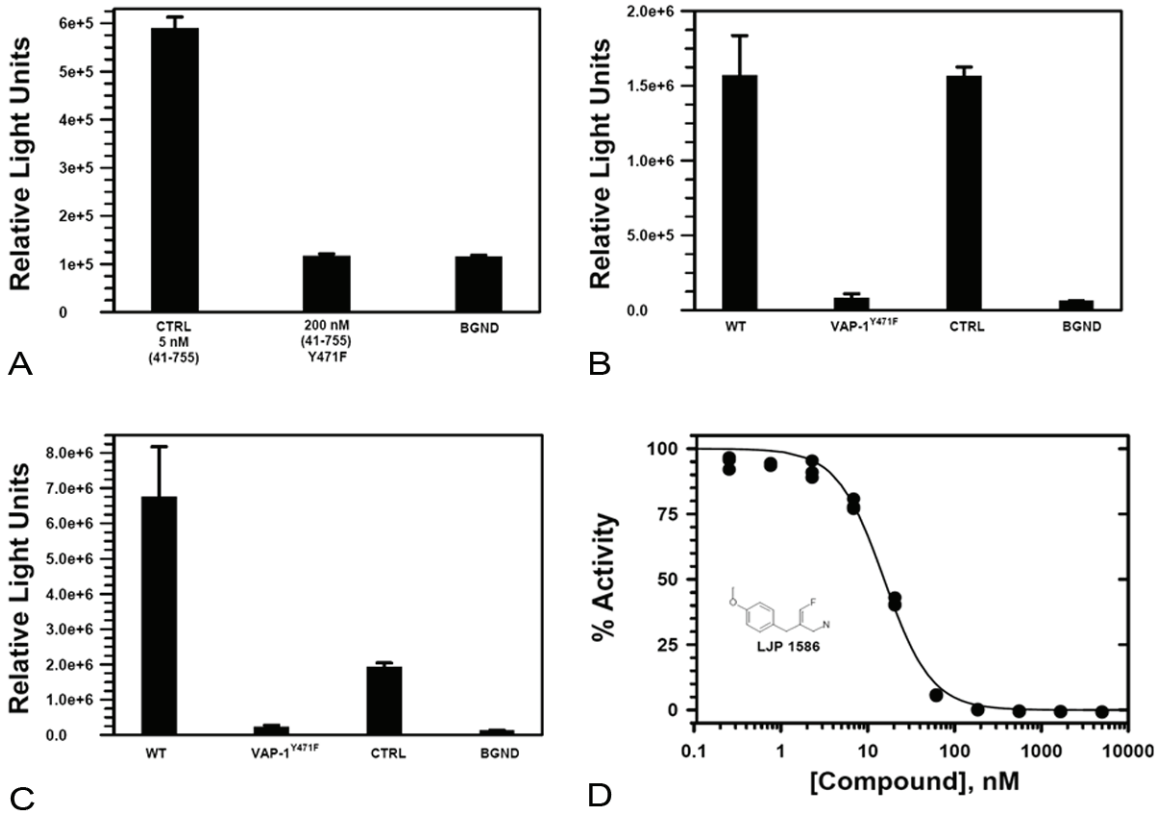

Figure 3. Ex vivo oxidase activity of wild type VAP-1 and VAP-1^{Y471F}. A: Human recombinant VAP-1 (41-755) (5 nM) and human recombinant VAP-1 (41-755)^{Y471F} (200 nM). (n=3) were assayed in a bioluminescent assay with a 60 min reaction time as outlined in the Materials and Methods. Relative light units (RLU) are indicated on the y axis. B: Wild type (WT) aorta (n=7 mice) and VAP-1^{Y471F} aorta (n=8 mice). Each sample included 48 µg total protein assayed in duplicate. 1 nM human recombinant VAP-1 (41-755) and samples without homogenate or enzyme (BGND) (both n=4) are also included. C: Adipose tissue homogenates (25 µg in quadruplicate) from wild type (WT) and VAP-1^{Y471F} mice (n=9 each) were assayed in the presence of 1 µM of both clorgyline and deprenyl. 1 nM human recombinant VAP-1 (41-755) and samples without homogenate or enzyme (BGND) (Both n=12) are also included. Bars represent averaged experimental data and error bars represent standard deviation. D: LJP1586 was assayed against wild type adipose homogenate (26 µg of protein pooled from 9 mice) and the IC_{50} was determined. Data are presented as a percentage of control activity with compound of interest, plus clorgyline & deprenyl (n=12). Symbols represent experimental data and are triplicate samples with backgrounds subtracted.

Table 1. Peripheral blood: Complete blood count and differential analysis

		Wild type mice (n=10)		VAP-1^{Y471F} (n=10)		
Parameter	Unit	Mean	+/- SD	Mean	+/- SD	*p* value
White blood cells	x 10^3/µL	10.6	1.9	13.6	4.4	0.263
Lymphocytes	x 10^3/µL	9.4	1.7	11.0	2.8	0.354
Monocytes	x 10^3/µL	0.5	0.1	1.0	0.4	0.055
Granulocytes	x 10^3/µL	0.8	0.3	1.6	1.2	0.259
Red blood cells	x 10^3/µL	8.67	0.2	8.36	0.4	0.202
Hemoglobin	g/dL	14.3	0.4	14.7	0.3	0.228
Hematocrit	%	47.4	2.7	46.8	2.9	0.763
Platelets	x 10^3/µL	1084	257	1138	180	0.742

Blood samples from ten VAP-1^{Y471F} and ten WT mice were analyzed by Beckman AcT Diff Coulter Counter. Mean Leukocyte and platelet counts are given in thousands, erythrocyte counts in millions along with standard deviation (SD) and the *p* value from unpaired Student's T test. Hemoglobin values are in grams/deciliter (g/dL) and hematocrit is in calculated percent.

Table 2. Flow cytometry evaluation of leukocyte populations in spleen and bone marrow

	Wild type mice (n=10)		VAP-1^{Y471F} (n=10)		
Bone marrow leukocytes CD45$^+$	Mean (%)	+/- SD	Mean (%)	+/- SD	*p* value
CD3$^+$	0.21	0.05	0.26	0.04	0.27
CD4$^+$	0.06	0.01	0.06	0.01	0.26
CD8$^+$	0.10	0.02	0.14	0.04	0.14
CD19$^+$	2.06	0.34	1.90	0.41	0.55
Gr1^{++} CD115$^-$ F4/80$^-$	5.34	0.22	10.26	3.03	0.05
CD115$^+$ Gr1$^{-/+}$	0.78	0.05	1.14	0.46	0.23
F4/80$^+$ Gr1$^{-/+}$	1.61	0.16	1.99	0.47	0.30
Spleen leukocytes (%)					
CD3$^+$	5.96	2.34	5.82	0.97	0.88
CD4$^+$	3.35	1.41	3.17	0.59	0.74
CD8$^+$	2.44	0.87	2.46	0.32	0.97
CD19$^+$	14.04	4.24	12.27	1.88	0.34

Cells isolated from the femur and tibia or spleens of four VAP-1^{Y471F} and four wild-type mice stained with fluorescently labeled antibodies to CD3, CD4, CD8, CD19, GR-1, F4/80, CD115 and analyzed by flow cytometry. Percentages of each cell type and total cell count were used to determine the number of each cell type (x 10^5). Mean, standard deviation (SD) and *p* value from unpaired Student's T test provided.

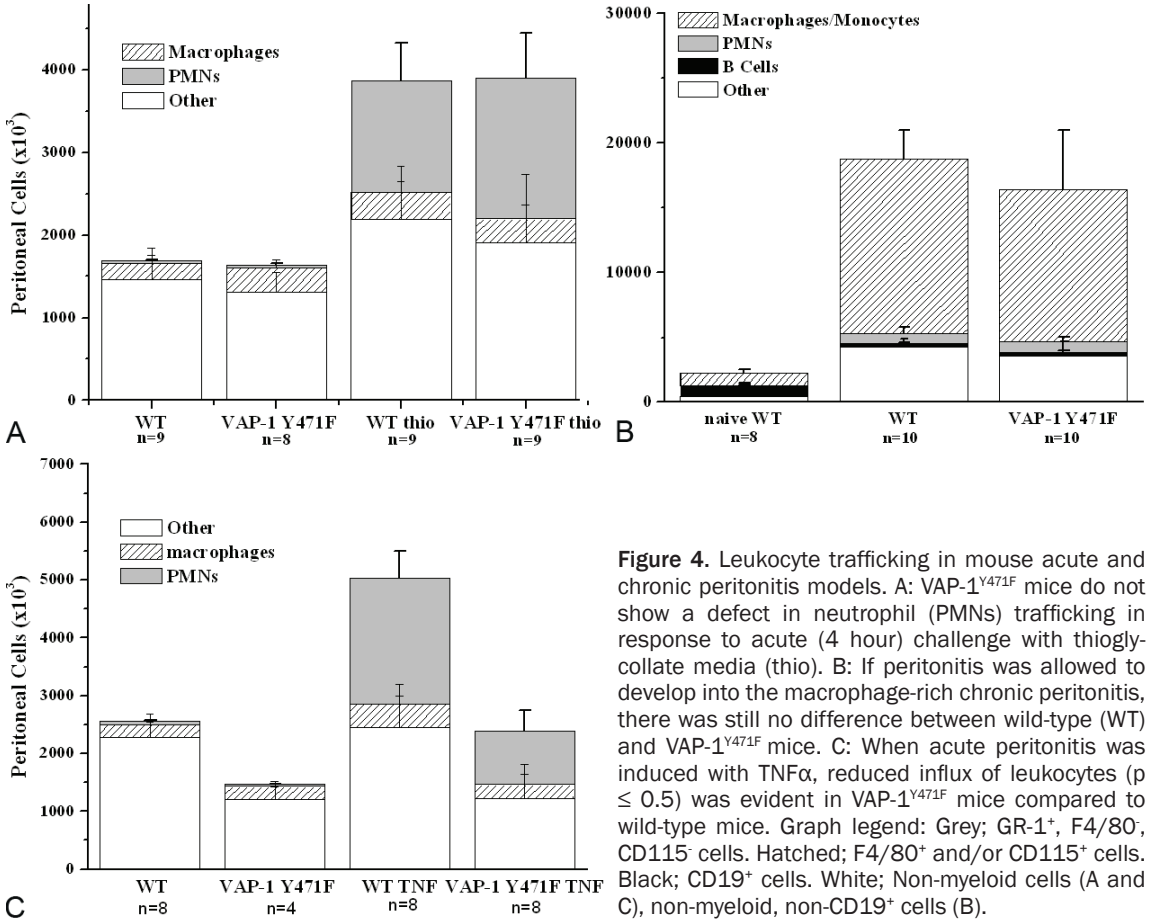

Figure 4. Leukocyte trafficking in mouse acute and chronic peritonitis models. A: VAP-1^{Y471F} mice do not show a defect in neutrophil (PMNs) trafficking in response to acute (4 hour) challenge with thioglycollate media (thio). B: If peritonitis was allowed to develop into the macrophage-rich chronic peritonitis, there was still no difference between wild-type (WT) and VAP-1^{Y471F} mice. C: When acute peritonitis was induced with TNFα, reduced influx of leukocytes ($p \leq 0.5$) was evident in VAP-1^{Y471F} mice compared to wild-type mice. Graph legend: Grey; GR-1$^+$, F4/80$^-$, CD115$^-$ cells. Hatched; F4/80$^+$ and/or CD115$^+$ cells. Black; CD19$^+$ cells. White; Non-myeloid cells (A and C), non-myeloid, non-CD19$^+$ cells (B).

(p=0.055, **Table 1**). There were also no differences in the calculated hematocrit or hemoglobin for VAP-1^{Y471F} mice.

The spleen and bone marrow from VAP-1^{Y471F} and WT animals were characterized by flow cytometry (CD3$^+$, CD4$^+$, CD8$^+$ and CD4$^+$CD8$^+$ T

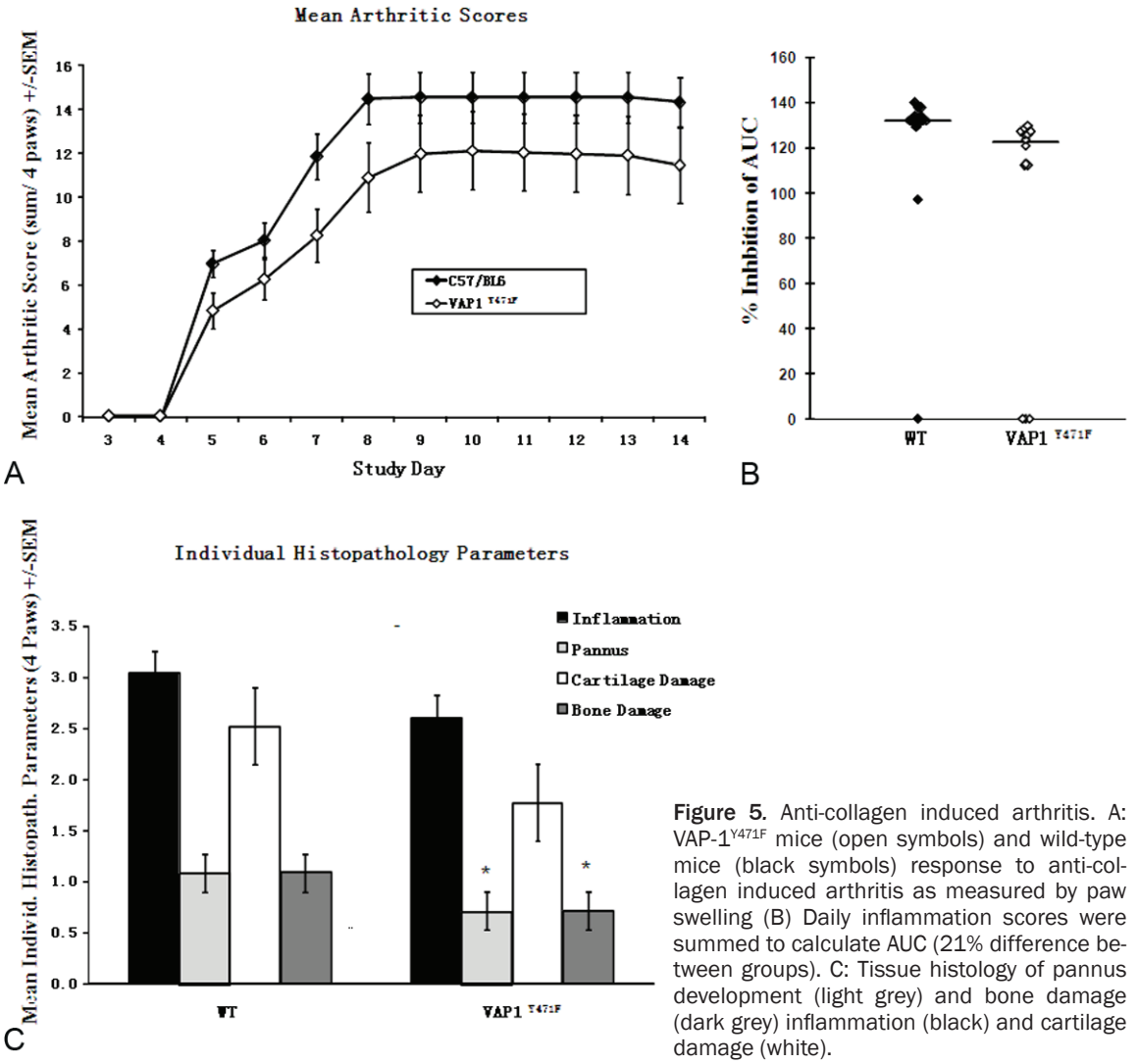

Figure 5. Anti-collagen induced arthritis. A: VAP-1^{Y471F} mice (open symbols) and wild-type mice (black symbols) response to anti-collagen induced arthritis as measured by paw swelling (B) Daily inflammation scores were summed to calculate AUC (21% difference between groups). C: Tissue histology of pannus development (light grey) and bone damage (dark grey) inflammation (black) and cartilage damage (white).

lymphocytes and CD19$^+$ B lymphocytes) and no significant differences were observed (**Table 2**). The bone marrow of VAP-1^{Y471F} mice contained two fold higher neutrophils than WT mice which may reflect a defect in exit of granulocytes in the absence of enzymatically active VAP-1. Macrophages (F4/80$^+$) and monocytes (CD115$^+$) were not significantly elevated in the bone marrow of VAP-1^{Y471F} mice (**Table 2**).

Evaluation of VAP-1^{Y471F} mice in models of cell trafficking and inflammation

The VAP-1^{Y471F} mice were evaluated in three different models of acute peritonitis; thioglycollate induced neutrophil recruitment (at 4 hrs), thioglycollate induced macrophage recruitment (at 72 hrs) and TNF induced neutrophil recruitment (at 6 hrs). Both naïve WT and VAP-1^{Y471F} mice had similar numbers of leukocytes recovered in the peritoneal wash (**Figure 4A**). GR-1$^+$ neutrophils were absent and F4/80$^+$ macrophages and CD115$^+$ monocytes were present in small numbers. VAP-1^{Y471F} mice did not demonstrate any deficit in neutrophil influx in response to stimulation with thioglycollate. Four hours after injection of thioglycollate media, there is an influx of neutrophils as defined by GR-1$^+$, F4/80$^-$, CD115$^-$ staining (**Figure 4A**). Similarly, the number of macrophages and monocytes in VAP-1^{Y471F} mice recovered 72 hrs after thioglycollate were the same as WT. The pattern of leukocytes isolated from peritoneal wash changed with some remaining GR-1$^+$ neutrophils and large numbers of F4/80$^+$ macrophages, many of which still also express

CD115 indicating monocytes differentiating into macrophages (**Figure 4B**). In this experiment CD19 was used to define B cells in the peritoneal wash showing that a significant portion of the peritoneal cells in naïve mice are B cells. Less $CD19^+$ cells are found at 72 hrs and again there were no differences between WT and VAP-1^{Y471F} (**Figure 4B**). However, when TNFα was used as the stimulus for acute peritonitis, there were 50% less neutrophils found at 6 hrs in the peritoneal wash of VAP-1^{Y471F} mice than WT (**Figure 4C**) similar to what has been observed for the VAP-1 null mice [17].

The response of VAP-1^{Y471F} mice was also tested in an Anti-type II Collagen Antibody Induced Arthritis (CAIA). Arthritis was induced in both VAP-1^{Y471F} and WT mice by injection of a cocktail of anti-collagen antibodies followed by a peritoneal injection of LPS. The time to onset of observable inflamed paws was the same in both WT and VAP-1^{Y471F} (**Figure 5A**). Both groups reached a plateau in the inflammation around day 8 and there was slightly less inflammation in VAP-1^{Y471F} (21% decrease in AUC) (**Figure 5B**). At the endpoint, the paws were fixed in formalin, sectioned and stained, and histological assessment was performed by a pathologist blinded to treatment (**Figure 5C**). There was no reduction in mean score for inflammation or cartilage damage but both pannus formation and bone damage were significantly less in VAP-1^{Y471F} compared to WT mice.

Discussion

A role for VAP-1 in mediating leukocyte migration and propagation of inflammation has been proposed to be facilitated by both its enzymatic activity [9] and direct adhesion, as demonstrated with blocking antibodies [18]. Previous investigators have demonstrated the importance of VAP-1 by generating knock-out mice lacking VAP-1 [17], however it is not clear if VAP-1 function is dependent on the oxidase activity or on other structural features of the protein. It is important to understand the contributions of each aspect of VAP-1 in order to correctly target it therapeutically. We sought to test the relative importance of these concepts *in vivo* by eliminating the oxidase activity but leaving the VAP-1 protein intact.

We therefore generated and characterized mice with an oxidase dead VAP-1 protein by making a point mutation in the active site of the protein (VAP-1^{Y471F}). We have shown that this mutant has no detectable oxidase activity as a recombinant protein *in vitro* and we confirmed that although the protein is expressed at comparable levels to the wild type protein *in vivo*, there is no detectable activity in all tissues analyzed where expression is high (e.g. aorta, lung, blood, adipose tissue). There are four SSAO family members in addition to VAP-1; AOC 1 (soluble), AOC 2 (retina specific) and AOC 4 (inactive pseudogene) and we evaluated their mRNA expression to look for changes in expression but none were observed.

Gross phenotypic analysis showed that the VAP-1^{Y471F} mice are viable, fertile and appear normal, including their hematological profile. There are slight differences in the numbers and ratios of cells in the VAP-1^{Y471F} mice compared to the VAP-1 KO mice, which most likely can be attributed to the establishment of the mice on different background strains (C57BL/6 vs S129). The only abnormal observations were slight weight gain as the animals get older, particularly in males, as described [19], and a defect in neutrophil trafficking under certain circumstances also described by [17] in the VAP-1 KO animals. The trafficking defect was demonstrated in a TNFα-induced sterile peritonitis model of neutrophil trafficking where VAP-1^{Y471F} mice had ~50% fewer neutrophils trafficking than WT mice. This is a subtle effect as thioglycollate induced trafficking to the peritoneum, of neutrophils at 4 hrs or monocyte/macrophages at 72 hrs [20], was normal in the VAP-1^{Y471F} mice. Thioglycollate stimulation is a more complex stimulus; it is a mixture of protein carbohydrate and electrolyte components that includes glycation end products which stimulate Receptors for Advanced Glycation End products (RAGE). Stimulation of RAGE induces inflammatory cascades that produce TNFα and other mediators including IL-6, MIP2α and activation of the NF-κB and activator protein-1 pathways [21-23]. Taken together, the results of thioglycollate-induced and the TNFα-induced peritonitis in VAP-1^{Y471F} mice, suggests that VAP-1 is important for TNFα-induced trafficking but not so important under other circumstances such as the response to thioglycollate media. TNFα is a major physiological player in this process of neutrophil trafficking, as illustrated by many studies including the use of

TNFα null mice. Stolen et al [17] reached a similar conclusion after finding clear evidence of a role for VAP-1 in TNFα peritonitis and also in a model of autoimmune diabetes using VAP-1 KO mice. The VAP-1 KO mice respond normally to bacterial infection [9].

The animals were further evaluated in an anti-collagen antibody-induced model of arthritis, as this model is less strain dependent than other models, avoids potential additional factors such as antigen presentation, lymphocyte homing and activation, and is a common model of rheumatiod arthritis in man. The anti-collagen antibody-induced arthritis model is dependent on PMNs, on complement fixation, and is relatively rapid in onset of inflammation [24]. This model also is enhanced when LPS is given three days after administration of the anti-collagen antibody cocktail which is known to induce TNFα release. Therefore this model depends on PMNs and TNFα, both of which we have shown to have modified responses in the VAP-1^{Y471F} mice.

The VAP-1^{Y471F} group of mice showed a slight decrease in inflammation as measured by AUC (21%) and histology compared to wild type mice. Several of the VAP-1^{Y471F} mice did not develop disease, and those that did develop disease showed slightly less severe inflammation compare to the wild type controls as highlighted by the histological evaluation. These results are very similar to those reported in VAP-1 KO mice [25] where on day 6 the clinical score per paw was approximately 40% less than WT littermates. These findings are consistent with a mild cell trafficking defect and are very similar to what was observed with the VAP-1 KO mice. Stolen et al. [17] utilized intravital microscopy to demonstrate that VAP-1 is important in mediating PMN rolling velocity, adherence, and transmigration in inflamed cremaster muscle, and also showed that anti-VAP-1 antibody had a similar effect. Some anti-VAP-1 antibodies (VAP-1 (TK8-14), Santa Cruz, sc-33670, VAP-1 clone 174-5 from HyCult Biotech (HM2213), and VAP-1 mouse mAb 7-88 (HyCult Biotech, HM1094) against human, mouse and rat did not inhibit enzymatic activity, tested up to 20 μg/mL, 10 μg/mL and 10 μg/mL, respectively, in our assay (data not shown, for methods see [12]). Stolen et al. [17] have also demonstrated reduced lymphocyte homing to peripheral lymph nodes and spleen. They attributed the partial reduction in PMN accumulation in VAP-1 KO mice to other adhesion molecules and observed further reduction in rolling flux in VAP-1 KO mice following administration of anti-L selectin.

There are several published reports of small molecule inhibitors of VAP-1 providing anti-inflammatory effects in animal models of inflammation [25-27]. These molecules are reactive hydrazines and irreversibly inhibit VAP-1 which can be very useful to define the role of VAP-1 inflammation. However, it is not clear how specific these molecules are and there may be covalent modification of other important proteins that affect inflammation and may explain the enhanced anti-inflammatory effect beyond what was found in VAP-1 KO mice [25]. Thus, the VAP-1^{Y471F} mice have allowed us to examine the enzymatic role of VAP-1 specifically.

Given the similarity of the VAP-1^{Y471F} mice and the VAP-1 KO mice phenotypes, our conclusion therefore is that VAP-1 activity is dependent on oxidase activity. This suggests that a small molecule, which inhibits the oxidase activity, would be sufficient to block VAP-1 effects *in vivo* and may have an impact on human disease. It further suggests that protein or antibody inhibitors of VAP-1 should block the active site in order to maximize their impact. Although the impact of VAP-1 is very limited in mouse models of arthritis, as shown in this work and with knockout animals, the VAP-1^{Y471F} mice represent a useful tool for estimating the impact of pharmacological inhibition of VAP-1 in a variety of other mouse models as investigators consider the relevant disease indications for VAP-1 inhibitors such as metabolic disease, atherosclerosis and fibrosis.

Non standard abbreviations

VAP-1, vascular adhesion protein-1; SSAO, semicarbazide-sensitive amine oxidase.

Acknowledgments

The authors gratefully acknowledge the contributions of Lynn Pantages and Mary McFarland in maintaining the animal colony.

Disclosure statement

All authors are employees of Boehringer Ingelheim Pharmaceuticals. All authors have

contributed to, read and approved the manuscript.

Address correspondence to: Dr. Louise Kelly Modis, Boehringer Ingelheim Pharmaceuticals, 900 Ridgebury Road, Ridgefield, CT 06877, USA. Phone: 203-791-6596. E-mail: Louise-Kelly.Modis@boehringer-ingelheim.com

References

[1] Lalor PF, Edwards S, McNab G, Salmi M, Jalkanen S, Adams DH. Vascular adhesion protein-1 mediates adhesion and transmigration of lymphocytes on human hepatic endothelial cells. J Immunol 2002; 169: 983-992.

[2] Smith DJ, Vainio PJ. Targeting vascular adhesion protein-1 to treat autoimmune and inflammatory diseases. Ann NY Acad Sci 2007; 1110: 382-388.

[3] Yraola F, García-Vicente S, Marti L, Albericio F, Zorzano A, Royo M. Understanding the mechanism of action of the novel SSAO substrate (C7NH10)6(V10028).2H20, a prodrug of peroxovanadate insulin mimetics. Chem Biol Drug Des 2007; 69: 423-8.

[4] Airas L, Mikkola J, Vainio JM, Elovaara I, Smith DJ. Elevated serum soluble vascular adhesion protein-1 (VAP-1) in patients with active relapsing remitting multiple sclerosis. J Neuroimmunol 2006; 177: 132-5.

[5] Madej A, Reich A, Orda A, Szepietowski JC. Vascular adhesion protein-1 (VAP-1) is overexpressed in psoriatic patients. J Eur Acad Dermatol Venereol 2007; 21: 72-8.

[6] Foot JS, Deodhar M, Turner CI, Yin P, van Dam EM, Silva DG, Olivieri A, Holt A, McDonald IA. The discovery and development of selective 3-fluoro-4-aryloxyallylamine inhibitors of the amine oxidase activity of semicarbazide-sensitive amine oxidase/vascular adhesion protein-1 (SSAO/VAP-1). Bioorg Med Chem Lett 2012; 22: 3935-40.

[7] O'Rourke AM, Wang EY, Miller A, Podar EM, Scheyhing K, Huang L, Kessler C, Gao H, Ton-Nu HT, MacDonald MT, Jones DS, Linnik MD. Anti-inflammatory effects of LJP 1586 [Z-3-Fluoro-2-(4-methoxybenzyl)allylamine Hydrochloride], an amine-based inhibitor of semicarbazide-sensitive amine oxidase activity. J Pharm Exp Ther 2008; 324: 867-875.

[8] Salmi M, Jalkanen S. A 90-kilodalton endothelial cell molecule mediating lymphocyte binding in humans. Science 1992; 257: 1407-9.

[9] Koskinen K, Vainio PJ, Smith DJ, Pihlavisto M, Ylä-Herttuala S, Jalkanen S, Salmi M. Granulocyte transmigration through endothelium is regulated by the oxidase activity of vascular adhesion protein (VAP-1). Blood 2004; 103: 3388-3395.

[10] Kivi E, Elima K, Aalto K, Nymalm Y, Auvinen K, Koivunen E, Otto DM, Crocker PR, Salminen TA, Salmi M, Jalkanen S. Human Siglec-10 can bind to vascular adhesion protein-1 and serves as its substrate. Blood 2009; 114: 5385-92.

[11] Aalto K, Autio A, Kiss EA, Elima K, Nymalm Y, Veres TZ, Marttila-Ichihara F, Elovaara H, Saanijoki T, Crocker PR, Maksimow M, Bligt E, Salminen TA, Salmi M, Roivainen A, Jalkanen S. Siglec-9 is a novel leukocyte ligand for vascular adhesion protein-1 and can be used in PET imaging of inflammation and cancer. Blood 2011; 118: 3725-33.

[12] Peet GW, Lukas S, Hill-Drzewi M, Martin L, Rybina IV, Roma T, Shoultz A, Zhu X, Cazacu D, Kronkaitis A, Baptiste A, Raudenbush BC, August EM, Modis LK. Bioluminescent method for assaying multiple semicarbazide-sensitive amine oxidase (SSAO) family members in both 96- and 384-well formats. J Biomol Screen 2011; 16: 1106-11.

[13] Holt A, Palcic MM. A peroxidase-coupled continuous absorbance plate-reader assay for flavin monoamine oxidases, copper-containing amine oxidases and related enzymes. Nature Protocols 2006; 1: 2498-2505.

[14] Chan J, Leenen PJ, Bertoncello I, Nishikawa SI, Hamilton JA. Macrophage Lineage Cells in Inflammation: Characterization by Colony-Stimulating Factor-1 (CSF-1) Receptor (c-Fms), ER-MP58, and ER-MP20 (Ly-6C) Expression. Blood 1998; 92: 1423-1431.

[15] Ziegler-Heitbrock L, Ancuta P, Crowe S, Dalod M, Grau V, Hart DN, Leenen PJ, Liu YJ, MacPherson G, Randolph GJ, Scherberich J, Schmitz J, Shortman K, Sozzani S, Strobl H, Zembala M, Austyn JM, Lutz MB. Nomenclature of monocytes and dendritic cells in blood. Blood 2010; 116: 74-80.

[16] Morin N, Lizcano JM, Fontana E, Marti L, Smih F, Rouet P, Prévot D, Zorzano A, Unzeta M, Carpéné C. Semicarbazide-sensitive amine oxidase substrates stimulate glucose transport and inhibit lipolysis in human adipocytes. J Pharmacol Exp Ther 2001; 297: 563-72.

[17] Stolen CM, Marttila-Ichihara F, Koskinen K, Yegutkin GG, Turja R, Bono P, Skurnik M, Hänninen A, Jalkanen S, Salmi M. Absence of the endothelial oxidase AOC 3 leads to abnormal leukocyte traffic in vivo. Immunity 2005; 22: 105-111.

[18] Salter-Cid LM, Wang E, O'Rourke AM, Miller A, Gao H, Huang L, Garcia A, Linnik MD. Anti-inflammatory effects of inhibiting the amine oxidase activity of semicarbazide-sensitive amine oxidase. J Pharmacol Exp Ther 2005; 315: 553-62.

[19] Bour S, Caspar-Bauguil S, Iffiú-Soltész Z, Nibbelink M, Cousin B, Miiluniemi M, Salmi M, Stolen C, Jalkanen S, Casteilla L, Pénicaud L, Valet P, Carpéné C. Semicarbazide-sensitive amine oxidase/vascular adhesion protein-1 deficiency reduces leukocyte infiltration into adipose tissue and favors fat deposition. Am J Pathol 2009; 174: 1075-83.

[20] Henderson RB, Hobbs JA, Mathies M, Hogg N. Rapid recruitment of inflammatory monocytes is independent of neutrophil migration. Blood 2003; 102: 328-335.

[21] Li YM, Mitsuhashi T, Wojciechowicz D, Shimizu N, Li J, Stitt A, He C, Banerjee D, Vlassara H. Molecular identity and cellular distribution of advanced glycation endproduct receptors: relationship of p60 to OST-48 and p90 to 80K-H membrane proteins. Proc Natl Acad Sci 1996; 93: 11047-52.

[22] Vlassara H, Li YM, Imani F, Wojciechowicz D, Yang Z, Liu FT, Cerami A. Identification of galectin-3 as a high-affinity binding protein for advanced glycation end products (AGE): a new member of the AGE-receptor complex. Mol Med 1995; 1: 634-646.

[23] Pullerits R, Brisslert M, Jonsson IM, Tarkowski A. Soluble receptor for advanced glycation end products triggers a proinflammatory cytokine cascade via beta2 integrin Mac-1. Arth Rheum 2006; 54: 3898-3907.

[24] Nadakumar KS and Holmdahl R. Antibody induced arthritis:disease mechanisms and genes involved at the effector phase of arthritis. Arthritis Res Ther 2006; 8: 223.

[25] Marttila-Ichihara F, Smith DJ, Stolen C, Yegutkin GG, Elima K, Mercier N, Kiviranta R, Pihlavisto M, Alaranta S, Pentikäinen U, Pentikäinen O, Fülöp F, Jalkanen S, Salmi M. Vascular amine oxidases are needed for leukocyte extravasation into inflamed joints in vivo. Arth Rheum 2006; 54: 2852-2862.

[26] Maytus P, Dajka-Halász B, Földi A, Haider N, Barlocco D, Magyar K. Semicarbazide-sensitive amine oxidase: current status and perspectives. Curr Med Chem 2004; 11: 1285-1298.

[27] Kiss J, Jalkanen S, Fülöp F, Savunen T, Salmi M. Ischemia-reperfusion injury is attenuated in VAP-1-deficient mice and by VAP-1 inhibitors. Eur J Immunol 2008; 38: 3041-3049.